Biotechnology & Biotechnological Equipment

ISSN: 1310-2818 (Print) 1314-3530 (Online) Journal homepage: https://www.tandfonline.com/loi/tbeq20

Antitumour activity of *Helix* hemocyanin against bladder carcinoma permanent cell lines

Aleksandar Dolashki, Pavlina Dolashka, Arnulf Stenzl, Stefan Stevanovic, Wilhelm K. Aicher, Lyudmila Velkova, Radostina Velikova & Wolfgang Voelter

To cite this article: Aleksandar Dolashki, Pavlina Dolashka, Arnulf Stenzl, Stefan Stevanovic, Wilhelm K. Aicher, Lyudmila Velkova, Radostina Velikova & Wolfgang Voelter (2019) Antitumour activity of *Helix* hemocyanin against bladder carcinoma permanent cell lines, Biotechnology & Biotechnological Equipment, 33:1, 20-32, DOI: 10.1080/13102818.2018.1507755

To link to this article: https://doi.org/10.1080/13102818.2018.1507755

Published online: 26 Jan 2019.

BIOTECHNOLOGY & BIOTECHNOLOGICAL EQUIPMENT
2019, VOL. 33, NO. 1, 20–32
https://doi.org/10.1080/13102818.2018.1507755

Antitumour activity of *Helix* hemocyanin against bladder carcinoma permanent cell lines

Aleksandar Dolashki[a], Pavlina Dolashka[a], Arnulf Stenzl[b], Stefan Stevanovic[c], Wilhelm K. Aicher[b], Lyudmila Velkova[a], Radostina Velikova[a] and Wolfgang Voelter[d]

[a]Institute of Organic Chemistry with Centre of Phytochemistry, Bulgarian Academy of Sciences, Sofia, Bulgaria; [b]Department of Urology, University of Tübingen Hospital, Tübingen, Germany; [c]Department of Immunology, Institute for Cell Biology, University of Tübingen, Tübingen, Germany; [d]Interfacultary Institute of Biochemistry, University of Tübingen, Tübingen, Germany

ABSTRACT

Hemocyanins are oxygen-transporting glycoproteins in molluscs and arthropods. In this study, we assayed the biomacromolecules from the molluscs *Helix lucorum* (HlH), *Rapana venosa* (RvH) and *Megatura crenulata* (KLH) including their functional units (FUs), for therapy of bladder cancer permanent cells. *In vitro* studies antitumour activities of these proteins were performed with bladder cancer permanent cell line CAL-29 and the normal urothelial cell line HL 10/29 in comparison to doxorubicin. The obtained results showed that the human tumour CAL-29 cell line is sensitive to the action of the tested hemocyanins and their isoforms. We observed a dose- and time-dependent inhibition of tumour cell growth after incubation with native HlH and two FUs (β_c-HlH-a and FU β_c-HlH-h); and of particular significance, FU β_c-HlH-h showed a surprisingly stronger effect than that the doxorubicin-treated cells. Cells treated with β_c-HlH-h, showed both, apoptotic and necrotic cells. In addition, two-dimensional polyacrylamide gel electrophoresis (PAGE) found for differential up-regulation of several proteins after hemocyanin treatment. Eight different down-regulated and two up-regulated proteins were identified, which may be associated with the apoptosis pathway. No inhibition of the normal urothelial cell line HL 10/29 was observed after treatment with HlH and its isoforms. The most effective inhibition of CAL-29 tumour cells was observed after treatment with β_c-HlH-h, probably caused by a specific oligosaccharide structure of HlH with methylated hexoses. These results suggest that hemocyanin glycosylation plays an important role in its anticancer activity.

Abbreviations: CCH: Concholepas concholepas hemocyanin; FLH: Fissurella latimarginata hemocyanin; FUs: Functional units; Hc: Hemocyanin; HlH: Helix lucorum hemocyanin; HvH: Helix vulgaris hemocyanin; KLH: keyhole limpet Megatura crenulata hemocyanin; LvH: Litopenaeus vannamei hemocyanin; βc-HlH: Structural subunit 'βc' of HlH; βc-HlH-a: Functional unit 'a' of HlH; βc-HlH-h: Functional unit 'h' of HlH; RvH1-c: Functional unit 'c' of RvH; RvH2-g: Functional unit 'g' of RvH; RvH: Rapana venosa hemocyanin; RvH1: 2 Structural subunits 1 and 2 of Rapana venosa hemocyanin; RvH1-c: Functional unit c of Rapana venosa hemocyanin

ARTICLE HISTORY
Received 22 November 2017
Revised 24 July 2018
Accepted 31 July 2018

KEYWORDS
Hemocyanin; *Helix lucorum*; human tumour CAL-29 cell line; FUs (βc-HlH-a; FU βc-HlH-h); proteomic analyses; apoptotic; necrotic cells

Introduction

Hemocyanins (Hcs), well-studied oligomeric glycometalloproteins carrying oxygen in the hemolymph of arthropod and mollusc species, differ largely in molecular masses, quaternary structures [1–5], carbohydrate content, and composition [6–8]. They have large molecular weights (from 4 up to 9 MDa) [4] and, due to their xenogenic nature, are strongly immunogenic. Activating the immune system of mammals [9–13], they stimulate innate immunity by inducing macrophage activation [9].

Hemocyanins are adjuvants for producing antibodies against different antigens in therapeutic vaccines against cancer [9–11] or against tumour antigens in generation of *ex vivo* autologous tumour cell lysate-loaded dendritic cells (DCs) to induce T-cell responses in cancer patients [9,12,13]. Hemocyanins have been used clinically as non-specific immunostimulants to prevent the progression of superficial bladder cancer, suggesting them ideal for longterm ongoing treatment [9,13,14].

The relevance of the glycosylation of hemocyanin isoforms KLH1 and KLH2 of *Megathura crenulata*

CONTACT Pavlina Dolashka pda54@abv.bg, Aleksandar Dolashki adolashki@yahoo.com Institute of Organic Chemistry with Centre of Phytochemistry, Bulgarian Academy of Sciences, Sofia, Bulgaria
Color versions of one or more of the figures in the article can be found online at www.tandfonline.com/tbeq.

[15–17] and the clinical success in patients with bladder carcinoma are assumed to be caused by a disaccharide epitope Gal(β1-3)GalNAc, cross-reacting with an epitope on the bladder tumour cell surface [17]. As reviewed earlier [11], the versatile biomedical and clinical applications of KLH have led to growing interest in finding new alternative hemocyanins with similar or more potent immunomodulatory, antimicrobial, and antiviral properties [18–21].

Several hemocyanins from other species of mollusks have significant immunological and antitumour potential, including *Concholepas concholepas* (CCH) [22] and *Fissurella latimarginata* (FLH) [23,24]. In vitro studies on the mechanism of the antiproliferative activity of the hemocyanin from shrimp Litopenaeus vannamei (LvH) against the most commonly used human HeLa cell line the innate immunity by inducing different temporal patterns of proinflammatory cytokine expressions in macrophages [25].

Our previous studies demonstrated that isoforms and functional units of hemocyanins from *Rapana venosa* (RvH) and *Helix lucorum* (HlH) (previously called *Helix vulgaris* (HvH)) have antitumor activity and immunological properties [26–28]. The results showed that both hemocyanins may be useful for the development of new antiviral, antibacterial and antitumour vaccines since they seem to launch strong and specific immune response against conjugated antigens [27].

As was reported recently, the molluscan hemocyanins HlH and RvH change the gene expression in human bladder cancer cells [28]. Bladder cancer is the second most common urological cancer, clinically characterized by a high recurrence rate and poor prognosis [28,29]. Moreover, approximately 20% of recurring bladder cancer cases can develop into muscle-invasive tumours [30]. Therefore, bladder cancer remains a focus in cancer research and several novel bladder cancer biomarkers have been identified [31].

It was demonstrated that RvH and Helix aspersa (HaH) have a direct antiproliferative effect on CAL-29 and T-24 bladder cancer cell lines, and the antitumour properties of HlH are superior to KLH [31,32]. Native HlH and the structural subunits from RvH are alternative candidates for the treatment of human superficial bladder cancer [33]. These findings lay the ground for more extensive studies on *Helix lucorum* hemocyanins as potential therapeutic agents against bladder cancer [34]. Moreover, the structure of HlH is significantly different from that of KLH [35,36]. Native *H. lucorum* hemocyanin consists of three different structural subunits, βc-HlH, αD-HlH and αN-HlH. Each subunit, ranging from 350 to 450 kDa, includes eight globular-folded domains known as functional units (FUs) with molecular masses of about 50–60 kDa [9,35,36]. The aim of the present study was to assay the antitumour effect of molluscan hemocyanin from garden snail *Helix lucorum* (HlH) on the human bladder cancer cell line CAL-29 by proteomics analysis.

Materials and methods

Materials

The hemolymph was collected from the foot of Bulgarian garden snail *H. lucorum* and the crude hemocyanin was isolated from the hemolymph as was described by Velkova et al. [36].

Purification of hemocyanins and FUs

The native *H. lucorum* hemocyanin was isolated from the hemolymph after centrifugation. The native of *H. aspersa* hemocyanin with a molecular mass of ∼9 MDa is present in the hemolymph as a-HaH and βc-HaH isoforms. βc-HaH is composed of only one subunit type (βc-subunit), and a-HaH is composed of two types of subunits (αN-HaH and αD-HaH). Three isoforms, one β-HlH and two α-HlH, were separated after precipitation or crystallisation during dialysis against sodium acetate buffer at low ionic strength as described by Velkova et al. [36]. The isoform βc-HaH was further analyzed by 5% native polyacrylamide gel electrophoresis, showing a single band with a mass of around 450 kDa [35].

R. venosa Hc was isolated from marine snails living in the Black Sea as described by Dolashka-Angelova et al. [36,37]. Eight functional units (FUs) were purified and analyzed by 7.5% or 10% sodium dodecyl sulphate (SDS)–polyacrylamide gel electrophoresis from the structural subunits of HlH and RvH [35–38].

Bladder cancer permanent cell lines

Experiments were carried out with commercially available permanent human CAL-29 tumour cell line (TCC), established from the primary lesion of a fatally invasive, metastatic TCC of the bladder (grade IV, stage T2) from an 80-year-old woman before treatment. After cultivation of CAL-29 cells in Dulbecco Modified Eagle's Medium (DMEM, Lonza, Austria), they were supplemented with 10% fetal bovine serum (Gibco, Austria), 100 U/mL penicillin, 0.1 mg/mL streptomycin, and 1% non-essential amino acids in 75-mL tissue culture plastic flasks (Falcon). Cells were maintained in

log growth phase at 37 °C in humidified air containing 5% CO_2.

Normal human urothelial cells were grown to confluence in complete keratinocyte serum-free medium (cKSFM) with human recombinant epithelial growth factor (5 ng/mL) bovine, pituitary extract (50 mg/mL; Gibco), supplemented with cholera toxin (30 ng/mL; List Biological Laboratories, Campbell, CA, USA) under standard conditions.

Determination of the antiproliferative activity of the tested hemocyanins

After washing with 0.1% EDTA/PBS (ethylenediaminetetraacetic acid/phosphate buffered saline) for 5 min, CAL-29 cells were trypsinized with TrypLE Express (Gibco), centrifuged for 5 min at 1500 *g*, and counted in a hemocytometer. Depending on the experimental need, cells were seeded at optimal inoculation density in well-plates or flasks and incubated overnight in expansion medium. Then cells were treated for 24, 48, and 72 h with various concentrations of the test substances glycosylated proteins: 150 μg/mL of the native of HlH (0.03 μmol/L), 150 and 300 μg/mL, with the structural subunit RvH1 (0.33 μmol/L and 0.66 μmol/L, respectively), and with the functional units (FUs) 150 and 300 μg/mL of β_c-HlH-a (3.0 μmol/L and 6.0 μmol/L), 150 μg/mL of β_c-HlH-h (3.0 μmol/L), 150 and 300 μg/mL of β_c-HlH-a (3.0 μmol/L and 6.0 μmol/L, respectively), 300 μg/mL RvH1-c (6.0 μmol/L) and compared to controls (= 100%), 150 μg/mL of KLH (0.03 μmol/L), and 0.1 μg/mL doxorubicin (DOX) (18.3 μmol/L) respectively. Doxorubicin served as positive control, medium as negative control. The effects of the substances on the cell viability were assessed by measuring the respiratory activity of mitochondria (WST-1-assay) and DNA synthesis (BrdU assay; both kits from Roche Diagnostics) using an ELISA plate reader (Milenia Kinetic Analyzer, Diagnostic Products). These analyses were performed two times. The percentage of cell growth inhibition was calculated as follows: $Cell\ viability\ (\%) = OD_{440}\ (experimental)/OD_{440}\ (control) \times 100$.

Statistical analysis

The data were processed using Exel and GraphPad Prism 5 and are presented as means with standard deviation (SD). Significance was tested using one-way analysis of variance (ANOVA) with Bonferroni adjustment for multiple comparisons. $p < .05$ was considered to indicate a statistically significant difference (shown in the figures as $^{*}p < .05$, $^{**}p < .01$ and $^{***}p < .001$ in comparison to a negative control, and $\hat{}p < .05$ and $\hat{}\hat{}p < .01$, in comparison to a positive control). The experiments were performed in triplicate and repeated at least three times.

Pro-apoptotic activity of hemocyanins

The induction of apoptosis was assessed after 24 h cultivation of CAL-29 tumour cells with 500 μg/mL HlH (0.08 μmol/L) and 500 μg/mL β_c-HlH-h (10 μmol/L) by the Annexin-V-FLUOS Kit (Roche, Diagnostics), and the results were compared with 0.1 mg/mL doxorubicin for positive and medium for the negative control. The cells were washed twice with PBS (Gibco) for 5 min and then covered with Annexin V labelling solution. After adding 1 μL of propidium iodide (PI) solution and 2 μL of fluorescein-annexin solution, the plates were incubated for 15 min at room temperature (15–20 °C) and then analyzed by fluorescent microscopy.

The cells were distinguished based on the following staining:

- Positive Annexin-V/FITC- staining is characteristic for apoptotic cells;
- Positive Annexin-V/FITC- and PI-staining is observed for late apoptotic or necrotic cells;
- Specific PI-staining is typical for necrotic cells.

Extraction of proteins from CAL-29 cells

The cells were washed two times with a blank medium without serum, which was then substituted with serum-free medium (SFM, Thermo Fisher). The cells were incubated for a further period of 24-hours, and the supernatant was collected for 2D-gel electrophoreses. Ten milligrams of lyophilised CAL-29 cells without treatment and after treatment with HlH were suspended in 50 mmol/L Tris-HCl, pH 7.5, 0.1 mmol/L EDTA and 1 mmol/L β-mercaptoethanol, and the mixtures were stirred for 45 min in a cold room. Then they were homogenized using a glass homogenizer and the homogenate is centrifuged at 12 000 × *g* for 20 min at 4 °C. The supernatants were stabilized with protease inhibitors (cocktail Roche) and 40% proteins were precipitated by gradually adding sufficient solid $(NH_4)_2SO_4$ (ultrapure reagent or enzyme grade). The precipitated protein was removed by centrifugation at 12 000 × *g* for 10 min, at 4 °C, and more $(NH_4)_2SO_4$ was added gradually to the supernatant to yield 80% saturation. After centrifugation, the fractions of precipitated proteins between 40 and 80% saturation

were resuspended gently in 10 mL of 20 mmol/L Tris-HCl buffer, pH 7.5, 20 mmol/L NaCl and 10 mmol/L $MgCl_2$, and dialyzed against 3 L of the same buffer to remove residual $(NH_4)_2SO_4$. The dialyzed suspension was centrifuged at 12 000 × *g* for 10 min, at 4 °C and the supernatants were analyzed by two-dimensional polyacrylamide gel electrophoresis (2D- PAGE).

2-DE analysis of proteins in CAL-29 tumour cells after treatment with HlH

After determination of the protein concentration of supernatants with the Protein Assay Kit (BioRad), approximately 250 μg of protein was mixed with IPG rehydration buffer (8 mol/L urea, 2% *w/v* CHAPS, 0.3% dithiothreitol (DTT), final volume of 360 μL). The strips were allowed to rehydrate for 7 h and to focus (IEF) using a Multiphor II system (Amersham Biosciences) running the following program: 150 V (30′), 150 V (120′), 300 V (30′), 300 V (45′), 3500 V (90′), 3500 V (540′), 500 V (10′), and held at 500 V. The temperature was kept at 18 °C. After completion of the IEF program, the IPG strips were equilibrated in a 50 m mol/L Tris-HCl solution, pH 8.8, containing 6 mol/L urea, 30% glycerol, 2% SDS, and 1% DTT, for 10 min, after which the solution was replaced with the same solution, except that DTT was exchanged by 5% iodoacetamide. The strips were placed on home-casted vertical SDS-PAGE gels and subjected to electrophoresis at 10 mA/gel for 15 min, followed by a 9-h run at 20 mA/gel until the bromophenol blue front reached the bottom of the gel. Staining was performed using Coomassie Brilliant Blue G-250 Dye (CBB G-250, Thermo Fisher Scientific). The 2D-gel images were digitized using a GS-710 densitometer (BioRad) and analyzed with the accompanying PDQuest 7.1 software (BioRad).

Analyses of proteins after gel guanidination and trypsin digestion of spots

Guanidination was performed by adding 5 μL of Milli-Q (MQ) water, 11 μL of 7 N ammonium hydroxide (Merck, Darmstadt, Germany), and 3 μL of a freshly prepared 7.5 mol/L *O*-methylisourea hemisulfate solution (Acros, Geel, Belgium) to the excised spots. The samples were vortexed briefly and incubated at 65 °C. After incubation for 2 h, the guanidinated samples were taken from the oven and the remainder of the solution was discarded. The gel pieces containing the guanidinated samples were desalted and destained in one step. Two washes using 150 μL of 200 mmol/L ammonium bicarbonate in 50% ACN/MQ (30 min at 30 °C) were performed and subsequently the gel pieces were dried in a SpeedVac (Thermo Savant, Holbrook, NY).

To reduce and alkylate the protein mixture prior to apply to trypsin digestion, 10 μL of 10 mmol/L DTT was added for 100 μL of the sample (5 μg/μL). The Eppendorf tube was incubated for 30 min at 60 °C. After being cooled down for 5 min to room temperature, 10 μL of 100 mmol/L iodoacetamide was added and the mixture was placed in the dark for 30 min. Then, 20 μL out of the 120 μL of the reduced and alkylated sample was digested. This sample was diluted in 60 μL of 0.1% SDS/50 mmol/L Tris (pH 7.4) and 20 μL of ACN and incubated overnight with 100 μL of 0.1 μg/μL trypsin (Promega, Madison, WI). The peptide mixture was dried in a SpeedVac. The sample was then dissolved in 20 μL of 0.1% formic acid.

A volume of 8 μL digestion buffer (50 mmol/L ammonium bicarbonate, pH 7.8) containing modified trypsin *per* microliter (Promega) was added to the dried gel spots and the tubes were kept on ice for 45 min to allow the gel pieces to be completely soaked with the protease solution. Digestion was performed overnight at 37 °C, the supernatants were recovered and the resulting peptides were extracted twice with 35 μL of 60% ACN/0.1% DIEA. The extracts were pooled and dried in the SpeedVac. The peptides were redissolved in 10 μL of 0.1% formic acid and matrix solution and spotted on the MALDI plate.

Protein identification by MS and MS/MS analyses

In all MALDI-MS and MS/MS applications, a 4800 plus MALDI TOF/TOF Analyzer (Applied Biosystems, Foster City, CA, USA) was used. Samples were prepared by mixing 0.7 μL of the sample with 0.7 μL matrix solution (7 mg/mL α-cyano-4-hydroxycinnamic acid (CHCA) in 50% ACN containing 0.1% TFA) and spotted on a stainless steel 192-well target plate. They were allowed to air dry at room temperature, and were then inserted in the mass spectrometer and subjected to mass analysis. The mass spectrometer was externally calibrated with a mixture of angiotensin I, Glu-fibrinopeptide B, ACTH (1–17), and ACTH (18–39). For MS/MS experiments, the instrument was externally calibrated with fragments of Glu-fibrinopeptide B. The search included fixed modification of acetyl (N-terminal peptide), acetyl-lysine and cysteine carbamidomethylation, variable modifications of methionine oxidation and deamidation of glutamine and asparagine. Protein identification based on MS/MS spectra was made against the Swiss-Prot database using an in-house

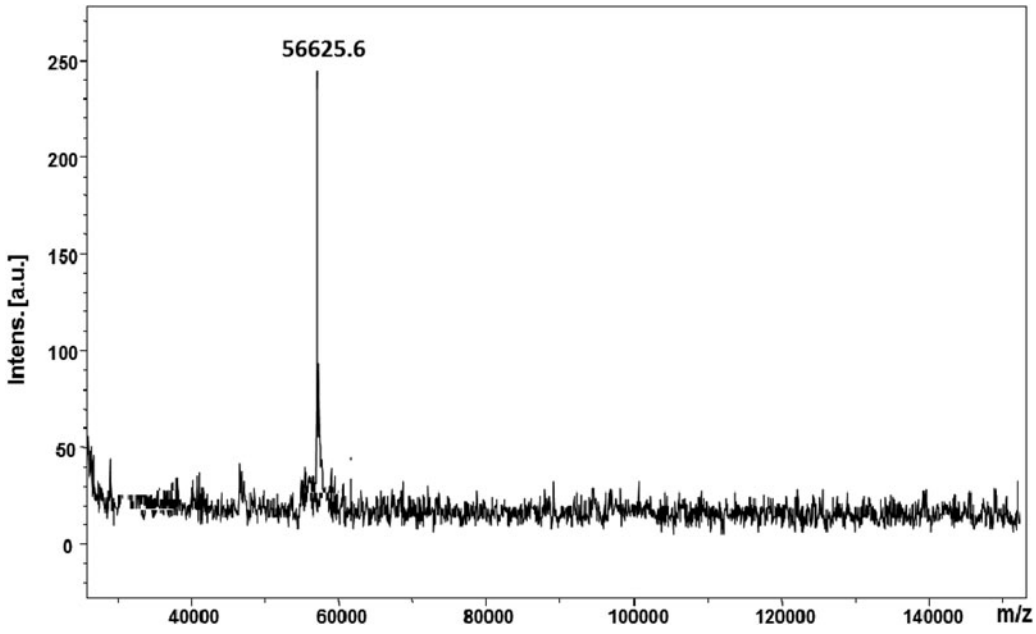

Figure 1. MALDI-MS spectrum of FU βc-HlH-h of *Helix lucorum* hemocyanin. Note: Human albumin (66347.7 Da) and rabbit actin (43 kDa) were used to calibrate the mass scale. The mass values assigned to the amino acid residues are average masses.

MASCOT server (Matrixscience, London, UK). Other restrictions to MASCOT were precursor ion *m/z* tolerance of ±0.3 Da, enzyme digestion with trypsin, up to one missed cleavage, and 1^+, 2^+ and 3^+ charged precursor ions were considered. The error for matching the daughter ions in the MS/MS spectra was 0.5 Da.

Database searches

Mass spectral data were searched against different protein databases using an in-house MASCOT server (Matrixscience, London, UK). NCBI BLAST-search was done with the amino acid sequences revealed by manual interpretation of the MS/MS spectra. *De novo* determined peptide sequences were deduced manually and used for similarity searches using the FASTS, MS-BLAST and the MS-Homology algorithm.

On-line submissions were performed using MS-BLAST at the Heidelberg server (http://dove.embl-heidelberg.de/Blast2/msblast.html). FASTS (http://fasta.bioch.virginia.edu/fasta_www/cgi/) was carried out using standard settings, and searches were performed against the NCBI/BLAST with BLOSUM 50 as the search matrix.

Results and discussion

In our preliminary study, we examined the antitumour effect of the native molluscan hemocyanins from the marine snail *R. venosa* and the garden snail *H. lucorum* and their subunits on CAL-29 and T-24 human bladder cancer cell line in comparison to compounds routinely used clinically, such as KLH, doxorubicin hydrochloride and mitomycin-C [27].

The experiments with HlH, RvH, RvH1 and RvH2 showed a direct growth inhibitory effect on the tumour cells mainly after treatment with native HlH, RvH and the structural subunit RvH1, at a concentration of 500 μg/mL as observed for KLH. Moreover, we found a stronger antitumoural effect of the functional unit RvH1-c against these tumour cells after a 24 hour for treatment, probably due to specific oligosaccharide structures exposed on the surface of the glycoprotein [38]. The mechanism of antitumour activity of HlH, βc-HlH-h, and RvH2-g hemocyanins includes induction of apoptosis [28]. In addition to the antiproliferative effect, gene expression profiling of the CAL-29 and T-24 cell line treated with HlH is associated with immune system activation, transcriptional misregulation and programmed cell death. The downregulated genes are associated with responses to wounding, lipopolysaccharide and angiogenesis [28].

Based on these results, we performed *in vitro* experiments to analyze the antitumour activities of the native hemocyanin from *H. lucorum* against CAL-29 tumour cells in comparison to its isoforms and get some insight into its mechanism of action on a molecular level. The native HlH, structural subunit and functional unit, were purified. The primary protein structures as well as the oligosaccharide compositions of two FUs from HlH (βc-HlH-h and βc-HlH-a) and one FU (RvH1-c) from RvH are well known. Therefore, we

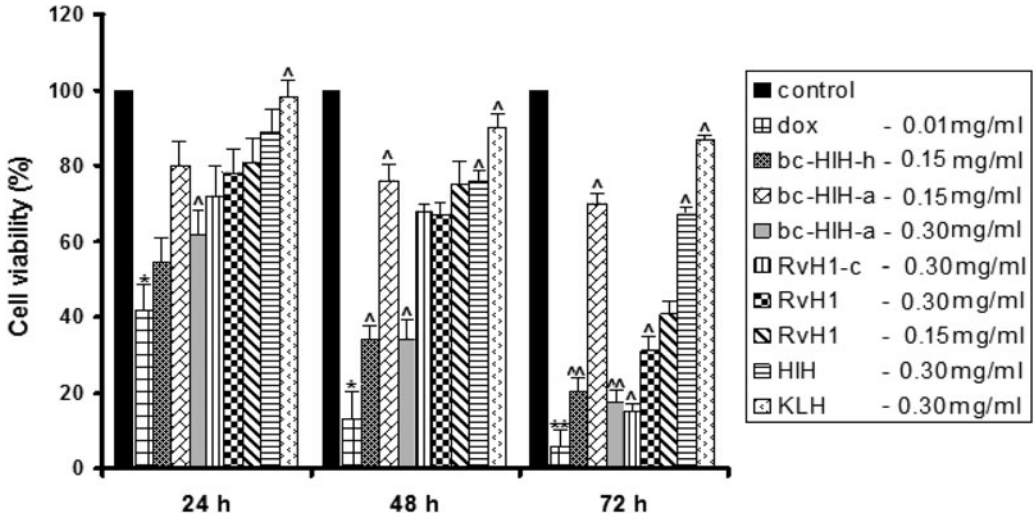

Figure 2. Effect of different doses of native HlH, structural subunit RvH1 and FUs of βc-HlH-h, βc-HlH-a, RvH1-c and KLH on the human tumour cell line CAL-29, after 24, 48 and 72 h of incubation, in comparison to negative and positive controls. Note: Native HlH molecule at 150 μg/mL (0.03 μmol/L); structural subunit RvH1 at 150 and 300 μg/mL (0.33 μmol/L and 0.66 μmol/L); FUs of βc-HlH-h at 150 μg/mL (3.0 μmol/L), βc-HlH-a at 150 and 300 μg/mL (3.0 μmol/L and 6.0 μmol/L), RvH1-c at 300 μg/mL (6.0 μmol/L) and KLH at 150 μg/mL (0.03 μmol/L). Medium alone (cells without treatment) was used as negative control; doxorubicin (DOX) at 0.1 μg/mL (18.3 μmol/L) was used as positive control. $^{*}p < .05$ and $^{**}p < .01$ in comparison to the negative control. $\hat{}p < .05$ and $\hat{}\hat{}p < .01$ in comparison to DOX.

analyzed their antitumour activities. The obtained isoforms were electrophoreticaly pure as confirmed by SDS-PAGE and MALDI-MS. The molecular mass of FU βc-HlH-h was determined to be 56625.6 $[M+H]^{+}$ as shown in the MALDI-MS spectrum (Figure 1).

Cytotoxic effect of hemocyanins

Hemocyanins (Hcs) may act as anti-proliferative agents on a variety of mammalian cells *in vitro* and *in vivo* [13,26,36,38]. However, the mechanisms involved in facilitating cell death by HlH and other Hcs have not been investigated in detail. We therefore, explored the antitumour activities of the native hemocyanin from *H. lucorum* against CAL-29 tumour cells in comparison to its isoforms to get some insight into its mechanism of action on a molecular basis.

Treatment of CAL-29 tumour cells with Hcs reduced the viability of the cells as determined by WST-assay (Figure 2). The inhibition of cell viability was dose- and time-dependent. After 72 hours of incubation, the respiratory activity of the cells was reduced to 67% with 300 μg/mL of HlH (0.06 μmol/L) and to 41% with 150 μg/mL of subunit RvH1 (0.33 μmol/L), compared to controls (100%). The cell viability drastically decreased after treatment of the tumour cells with 150 μg/mL of βc-HlH-h (3.0 μmol/L) (20.3%) and with 300 μg/mL of βc-HlH-a (6.0 μmol/L) (17.47%). For both FUs, βc-HlH-h and βc-HlH-a, this inhibition was stronger compared to the effect of native HlH and the structural subunit RvH1. HlH and RvH1 are more active than KLH (87%).

There were alterations of the CAL-29 cells' morphology after 24 and 48 h of treatment with 150 μg/mL (3.0 μmol/L) of both β_c-HlH-h and RvH1-c. Treatment with doxorubicin (0.1 mg/mL) served as control (Figure 3).

Comparison of the actions of the native molecules with the FUs from HlH and RvH showed that treatment with FUs more effective. FUs were purified and analyzed by 10% SDS–PAGE (data not shown). They induced significant inhibition on tumour cell growth and at the same time caused comparatively low effects on the metabolism and proliferation of normal cells (Figure 4(A)). This effect is probably due to specific oligosaccharide structures of these molecules, which are more accessible in the FUs of HlH [37] than the native molecules. The oligosaccharide structures of HlH are known and a mechanism of inhibition of tumour cell growth is suggested specific glycosylation sites of HlH and its FUs to interact with the target cells.

There are several reports on the interaction of glycosylation moieties of molluscan hemocyanins with the target cells. It is assumed that the clinical success of intravesical administration of KLH to patients with bladder carcinoma is based on the cross-reactivity of the disaccharide epitope Gal (β1-3)GalNAc with corresponding epitope on the bladder tumour cell surface [17].

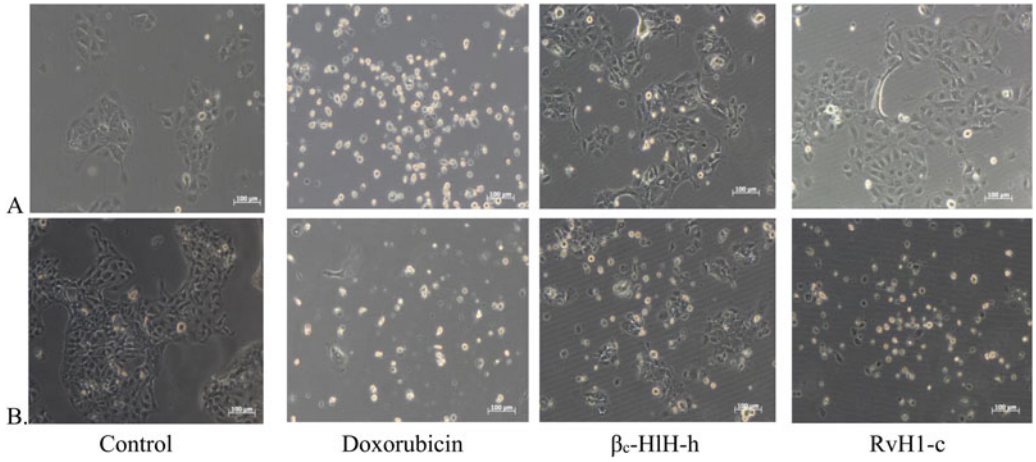

Figure 3. Morphological alterations of CAL-29 tumor cells treated for 24 h (A) and 48 h (B) with 0.1 μg/mL of doxorubicin (18.3 μmol/L) and 150 μg/mL (3.0 μmol/L) of FUs β_c-HlH-h and RvH1-c. Note: Untreated cells served as controls.

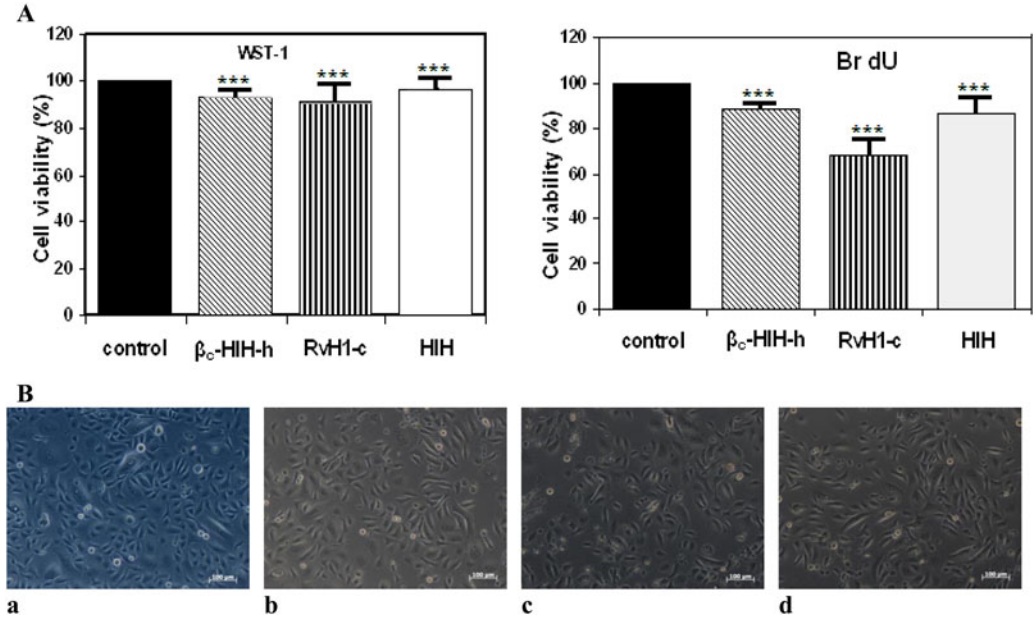

Figure 4. Cell viability (A) and morphological alterations (B) of HL 10/29 urothelial cells: untreated control cells (a) vs. cells treated for 48 h with 150 μg/mL (3.0 μmol/L) of β_c-HlH-h (b), RvH1-c (c) and native HlH (d). Note: $^{***}p < .001$ in comparison to the negative control.

To evaluate and compare the effect of the tested hemocyanins on normal urothelial cells HL 10/29, the tests were carried out with the lowest concentration of samples effective in arresting tumour cell growth. The data in Figure 3(B) show slight inhibition of metabolic activity and proliferation of the normal urothelial cells after treatment with 150 μg/mL of native HlH (0.03 μmol/L) and 150 μg/mL (3.0 μmol/L) of FUs β_c-HlH-h and RvH1-c on HL 10/29 urothelial cells after 48 h. Microscopy of HL 10/29 urothelial cells 24 hours after treatment with these samples demonstrated no visible alterations in the normal cell morphology in urothelial cultures (Figure 4(B)).

Analysis of cell death by fluorescence microscopy

The objective of anti-cancer therapy is to eliminate cancer cells from the body and also to prevent them from spreading to other parts of the organism. There are two major approaches: to limit tumour growth, i.e. limit the proliferation of tumour cells, or to induce apoptosis, the controlled death of tumour cells. The study of these two processes, apoptosis and proliferation of tumour cells, is the basis for the developments of new drugs and therapeutic approaches. Representative fluorescent morphologies of CAL-29 transitional carcinoma cell line after 24-h incubation with doxorubicin, HlH and β_c-HlH-h, are shown in

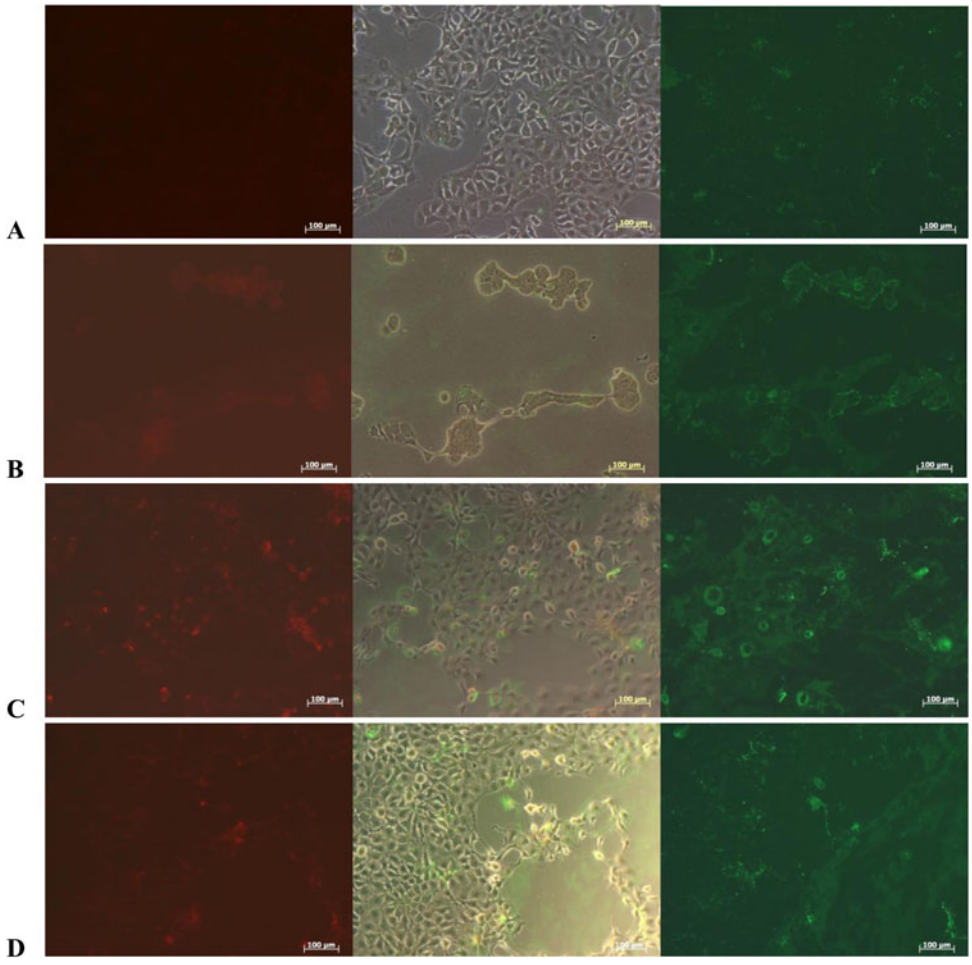

Figure 5. Fluorescence of CAL-29 bladder transitional cancer cells line recorded with green filter to detect apoptotic cells by binding of Annexin-V-FLUOS Kit (*right panel*) and nuclei of necrotic cells by PI (*left panel*) in the red channel. Phase contrast of the same area (*middle panel*) documented the culture density and cellular appearance. Micrographs were taken after 24 h of incubation of CAL-29 in (A) DMEM, at 37 °C and 5% CO_2 without treatment (controls); under the same conditions in medium as in (A) but complemented with (B) doxorubicin (183 μmol/L) or (C) 500 μg/mL of HlH (0.08 μmol/L) and (D) 500 μg/mL of β_c-HlH-h (10 μmol/L), respectively.

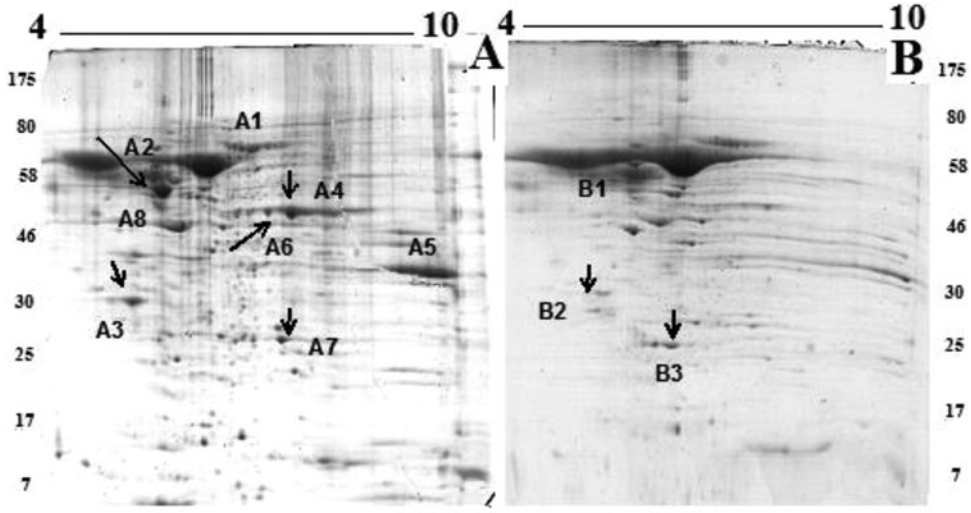

Figure 6. 2D-PAGE of pI 4–10 proteins from CAL-29 tumour cells: not treated (A) and treated (B) with HlH (pI 4–7, 12.5% acrylamide). Note: Annotated numbers refer to the identification of the proteins in Table 1.

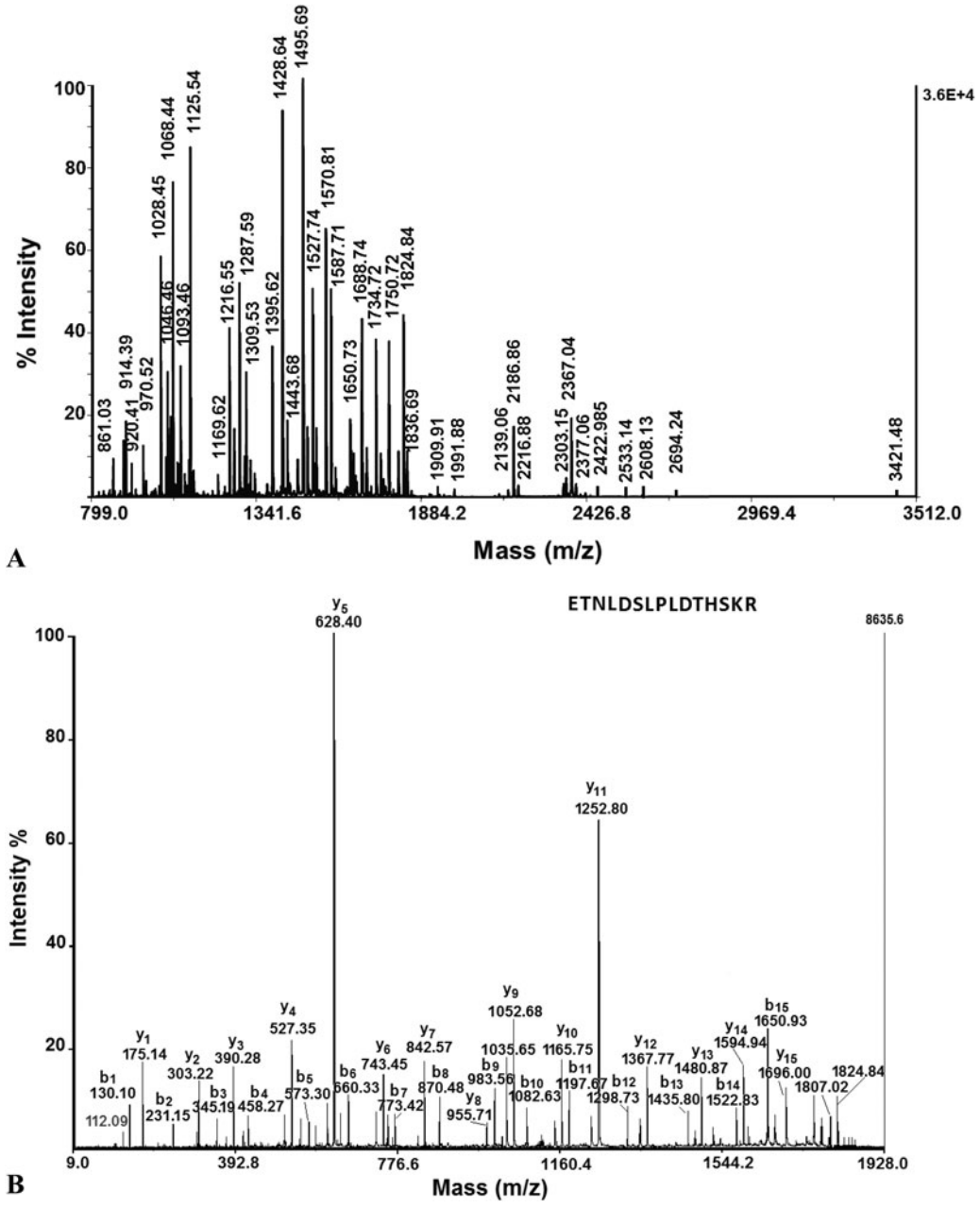

Figure 7. MS spectrum (A) of peptides obtained after trypsinolysis of protein on spot A2 from 2D-PAGE; (B) MS/MS spectrum from MALDI-TOF-TOF analysis of peptide at *m/z* 1824.84 from spot A2 of 2D-electrophoresis (protein Vimentin (VIME_HUMAN) with mass 53 676Da).

Figure 5. To identify, if native HlH and FU β_c-HlH-h induced reduction in the viability of CAL-29 tumour cells *via* apoptosis, the cells were stained with Annexin-V and the nuclei were co-stained with PI after 24-h incubation with 0.5 mg/mL of both samples. The adherent cells were detected by phase contrast microscopy (Figure 5). In the untreated controls, only very few cells were stained with Annexin-V, thus delivering a weak green signal. Moreover, red nuclear signals indicating dead cells were not observed for control cells (Figure 5(A)). In contrast, the doxorubicin-treated culture showed massive detachment and loss of cells in the phase contrast micrographs, strong binding of Annexin-V to most of the remaining cell membranes, but a low red nuclear PI signal, indicating that the cellular structure was dissolved to large parts and cells had probably undergone apoptosis (Figure 5(B)). A comparable effect was observed after treatment of CAL-29 tumour cells with Hcs. Strong binding of Annexin-V was detected after treatment of the cells with HlH, while the red fluorescence of PI remained low in most cells (Figure 5(C)). PI-positive nuclei correlated with round cells observed by phase contrast microscopy, indicating that most cells were

Table 1. Amino acid sequences of tryptic peptides of several spots from 2D-PAGE images, determined by MS/MS-analyses.

Spot	AAS of peptide	Mass $[M+H]^+$	Spot	AAS of peptide	Mass $[M+H]^+$
A1	LVNEVTEFAK	1149.60	**A6**	LGMFNIQHCK	1190.64
	AVMDDFAAFVEK	1342.53		PFVFLMIEQNTK	1466.76
	CCAAADPHECYAK	1381.56		DTVFALVNYIFFK	1576.86
	PCFSALEVDETYVPK	1697.92		ITPNLAEFAFSLYR	1641.89
	VPQVSTPTLVEVSR	1511.80		FNKPFVFLMIEQNTK	1855.99
	VHTECCHGDLLECADDR	1915.98		DTEEEDFHVDQVTTVK	1891.92
	WVTFISLLFLFSSAYSR	2037.38			
A2	EYQDLLNVK	1121.51	**A7**	ADGLAVIGVLMK	1186.70
	MALDIEIATYR	1295.52		MASPDWGYDDK	1284.58
	SLYASSPGGVYATR	1428.64		ESISVSSEQLAQFR	1580.75
	TYSLGSALRPSTSR	1495.69		YSAELHVAHWNSAK	1612.80
	ISLPLPNFSSLNLR	1570.81		LYPIANGNNQSPVDIK	1742.91
	ETNLDSLPLVDTHSKR	1824.84			
A3	ESTTSEQSAR	1095.35	**A8**	HTLNQIDEVK	1196.68
	GLCGAIHSSIAK	1156.45		CDSSPDSAEDVR	1280.55
	THSDQFLVAFK	1292.62		EHAVEGDCDFQLLK	1603.78
	IYGLGSLALYEK	1326.67		VCQDCPLLAPLNDTR	1657.86 2081.30
	AGVAGLSAWTLQPQWIQVR	2081.12		HTFMGVVSLGSPSGEVSHPR	
A4	IGAEVYHNLK	1143.55	**B2**	ATEHLSTLSEK	1215.64
	LMIEMDGTENK	1280.58		QGLLPVLESFK	1230.75
	YISPDQLADLYK	1425.72		DYVSQFEGSALGK	1400.74
	LAQANGWGVMVSHR	1525.75		AAVLTLAVLFLTGSQAR	1731.10
	AAVPSGASTGIYEALELR	1804.95			
A5	VVDLMAHMASK	1201.62 1411.78	**B3**	MLLADQGQSWK	1276.51
	GALQNIIPASTGAAK	1473.75		MPPYTVVYFPVR	1468.80
	VPTANVSVVDLTCR	1613.95		YISLIYTNYEAGK	1534.73
	LVINGNPITIFQER	1763.81		AFLASPEYVNLPINGNGK	1904.10
	LISWYDNEFGYSNR			ALPGQLQPFETLLSQNQGGK	2126.40

Table 2. Proteins with significant changes in abundance on 2D-gel PAGE before and after 48 h of treatment of CAL-29 cells with HlH.

Spot[a]	Name	UniProt KB:	UniGene	Gene name/GeneID	Mass (kDa)
A1	Serum albumin (ALBU_HUMAN)	*P02768*	Hs.418167 Hs.592379	ALB/GeneID:213.	69.367
A2	Vimentin [Homo sapiens (Human)] (VIME_HUMAN)	*P08670*	Hs.455493 Hs.691131	VIM/ GeneID:7431	53.6
A3	ATP synthase subunit gamma, mitochondrial (ATPG_HUMAN)	*P36542*	Hs.271135	ATP5C1/ GeneID: 509	32.996
A4	Alpha-enolase [Homo sapiens (Human)	*P067331*	Hs.517145	ENO1/ GeneID:2023	47.169
A5	Glyceraldehyde-3-phosphate dehydrogenase (Homo sapiens (Human)) (G3P_HUMAN, GAPDH)	*P04406*	Hs.544577 Hs.592355	GAPDH /GeneID:2597	36.053
A6	Alpha-1-antitrypsin (A1AT_HUMAN)	*P01009*	Hs.525557	SERPINA1/GeneID: 5265	46.737
A7	Carbonic anhydrase 1 (CAH1_HUMAN)	*P00915*	Hs.23118	CA1/GeneID: 759.	28.870
A8	Human alpha 2-HS-glycoprotein (Alpha-2-Z-globulin) AHSG	*P02765*	Hs.324746	AHSG /GeneID:197	49.0
B2	Apolipoprotein A-I [Homo sapiens(human)] (APOA1_HUMAN)	**P02647**	Hs.93194	APOA1/GeneID:335	30.778
B3	Glutathione S-transferase P (GSTP1_HUMAN)	**P09211**	Hs.523836	GSTP1/GeneID:2950	23.36

[a]Spot ID numbers in boldface (with the function of the corresponding protein) refer to the proteins with increased abundance and those in italics (with the corresponding function) to proteins with decreased abundance.

undergoing apoptosis (Figure 5(C)). Again, mostly apoptotic and a few necrotic cells were observed after treatment of CAL-29 with FU β_c-HlH-h as well (Figure 5(D)). Zheng et al. [25] described an *in vitro* effect of hemocyanin from *L. vannamei* against HeLa cell growth and the molecular mechanisms underpinning the antiproliferative effect of FLH was suggested to be a mitochondria-mediated apoptosis pathway.

These reports were supported by our data obtained from the tests for cytotoxic activity of hemocyanins and their isoforms. We observed a significant influence of Hcs on cell viability, which is in correlation with the processes of cell death, and it is possible that hemocyanins could be involved in the induction of cell death *via* different pathways.

Proteomic analysis of untreated CAL-29 cells and cells treatmed with HlH

Figure 2 shows that 72-h incubation with 300 μg/mL (0.03 μmol/L) of native *H. lucorum* Hc reduced the cell viability of CAL-29 tumour cells to 67%. To get more

insight into the mechanism of HlH inhibition on CAL-29 tumour cells, we performed the proteomic analysis. The proteins were extracted from untreated CAL-29 tumour cells and cells treated with HlH and were analyzed by 2D-gel SDS PAGE using a pH gradient from 4–7. A comparison of the proteins extracted from CAL-29 tumour cells (Figure 6(A)) with the proteins extracted after treatment with HlH (Figure 6(B)) revealed in a number of different protein spots. In addition, 2D PAGE detected differential upregulation (spots B2, B3) and downregulation (spots A1, A2, A3, A4, A6, A7, A8) of several proteins after hemocyanin treatment.

All differential spots were subjected to mass spectrometric analysis. The peptide mass fingerprint and MS/MS database search against the public protein databases did not facilitate an identification of the proteins. Therefore, they were identified by MS/MS analyses, Peaks studio and Mascot. The quality of 10 MS/MS spectra of tryptic peptides was sufficient to reveal 10 protein fragment sequences. Figure 7(A) shows an MS spectrum of the peptides obtained after trypsinolysis of proteins from spot A2 of the 2D-PAGE. The peptide at *m/z* 1824.84 was analyzed by MS/MS and the sequence determined as follows: ETNLDSLPLVDTHSKR (Figure 7(B)). Five different peptides extracted from spot A2 were identified by their MS/MS spectra and their sequences are presented in Table 1. A search in the protein sequence using NCBI BLAST showed amino acid sequences highly similar to the protein vimentin (VIME_HUMAN) with a mass of 53676 Da [39]. By this method, 10 different proteins were successfully identified: spot A1: serum albumin from urine samples[40], spot A2: vimentin [*Homo sapiens*] [41]; spot A3: ATP-phosphoribo-syltransferase [42]; spot A4: alpha-enolase [*Homo sapiens*][43]**;** spot A5: Glyceraldehyde-3-phosphate dehydrogenase (*Homo sapiens*)[44]; spot A6: alpha-1-antitrypsin (A1AT_HUMAN) [45]; spot A7: carbonic anhydrase 1 (CAH1_HUMAN)[46]; and spot A8: human alpha 2-HS-glycoprotein [47]. Figure 6(B) shows an increase in the expression of two proteins: B3 spot: glutathione S-transferase P1 [48] and Spot B2: apolipoprotein A-I [*Homo sapiens* (human)] [48,49]. Table 2 lists the identified proteins grouped by function in the main known metabolic pathways.

Conclusions

The observed results demonstrate that HlH, unlike KLH, shows potent antitumour activity on CAL-29 tumour cells. Moreover, the treatment with the FUs β_c-HlH-h and RvH1-c is more effective in comparison to native HlH. The mechanism of antitumour activity of HlH, β_c-HlH-h, and RvH2-c hemocyanins includes induction of apoptosis. The present study is the first report of protein expression in CAL-29 human cells under the influence of *H. lucorum* hemocyanin. Thus, the data provide an initial roadmap for further in-depth investigations into the mechanism of action of these proteins, thus supporting their application, especially as potential therapeutic agents against bladder cancer.

Disclosure statement

No potential conflict of interest was reported by the authors.

Funding

This work was supported by the Bulgarian Academy of Sciences under grant number DFNP-17-64/26.07.2017 for young scientists.

References

[1] Decker H, Hellmann N, Jaenicke E, et al. Minireview: recent progress in hemocyanin research. Integr Comp Biol. 2007;47(4):631–644.
[2] Markl J. Evolution of molluscan hemocyanin structures. Biochim Biophys Acta. 2013;1834(9):1840–1852.
[3] Gatsogiannis C, Hofnagel O, Markl J, et al. Structure of mega-hemocyanin reveals protein origami in snails. Structure. 2015;23(1): 93–103.
[4] Dolashka P, Zal F, Dolashki A, et al. ESI-MS and MALLS analysis of quaternary structure of molluscan hemocyanins. J Mass Spectrom. 2012;47(7):940–947.
[5] Wu J, Cunningham AL, Dehghani F, et al. Comparison of *Haliotis rubra* hemocyanin isoforms 1 and 2. Gene Reports. 2016;4:123–130.
[6] Sandra K, Dolashka-Angelova P, Devreese B, et al. New insights in *Rapana venosa* hemocyanin N-glycosylation resulting from on-line mass spectrometric analyses. Glycobiology. 2006;17(2):141–156.
[7] Dolashka P, Velkova L, Shishkov S, et al. Glycan structures and antiviral effect of the structural subunit RvH2 of Rapana hemocyanin. Carbohydr Res. 2010;345(16):2361–2367.
[8] Wuhrer M, Robijn ML, Koeleman CA, et al. A novel Gal(beta1-4)Gal(beta1-4)Fuc(alpha1-6)-core modification attached to the proximal N-acetylglucosamine of keyhole limpet haemocyanin (KLH) N-glycans. Biochem J. 2004;378(Pt 2):625–632.
[9] Becker MI, Arancibia S, Salazar F, et al. Mollusk hemocyanins as natural immunostimulants in biomedical applications. In: Huynh G, Duc T, editors. Immune response activation. Rijeka (Croatia): InTech; 2014. DOI: 10.5772/57552

[10] Del Campo M, Arancibia S, Nova E, et al. Hemocyanins as immunostimulants. Rev Med Chil. 2011;139(2):236–246.
[11] Arancibia S, Salazar F, Becker MI. Hemocyanins in the immunotherapy of superficial bladder cancer. In: Canda A, editor. Bladder cancer-from basic science to robotic surgery. Rijeka (Croatia): InTech; 2012. DOI: 10.5772/10
[12] Coates CJ, Decker H. Immunological properties of oxygen-transport proteins: hemoglobin, hemocyanin and hemerythrin. Cell Mol Life Sci. 2017;74(2):293–317.
[13] Lammers RJ, Witjes WP, Janzing-Pastors MH, et al. Intracutaneous and intravesical immunotherapy with keyhole limpet hemocyanin compared with intravesical mitomycin in patients with non–muscle-invasive bladder cancer: results from a prospective randomized phase III trial. J Clin Oncol. 2012;30(18):2273–2279.
[14] Krug LM, Ragupathi G, Hood C, et al. Vaccination of patients with small-cell lung cancer with synthetic fucosyl GM-1 conjugated to keyhole limpet hemocyanin. Clin Cancer Res. 2004;10(18 Pt 1):6094–6100.
[15] Lamm DL, Dehaven JI, Riggs DR. Keyhole limpet hemocyanin immunotherapy of bladder cancer: laboratory and clinical studies. European urology. 2000;37(Suppl.3):41–44.
[16] Markl J, Lieb B, Gebauer W, et al. Marine tumor vaccine carriers: structure of the molluscan hemocyanins KLH and HtH. J Cancer Res Clin Oncol. 2001;127(Suppl.2):R3–9.
[17] Kurokawa T, Wuhrer M, Lochnit G, et al. Hemocyanin from the keyhole limpet Megathura crenulata (KLH) carries a novel type of N-glycans with Gal(beta1-6)Man-motifs . Eur J Biochem. 2002;269(22):5459–5473.
[18] Coates CJ, Nairn J. Diverse immune functions of hemocyanins. Dev Comp Immunol. 2014;45(1):43–55.
[19] Dolashka-Angelova P, Lieb B, Velkova L, et al. Identification of glycosylated sites in Rapana hemocyanin by mass spectrometry and gene sequence, and their antiviral effect. Bioconjugate chemistry. 2009;20(7):1315–1322.
[20] Dolashka P, Voelter W. Antiviral activity of hemocyanins. Invertebr Surviv J. 2013;10:120–127.
[21] Dolashka P, Dolashki A, Beeumen JV, et al. Antimicrobial activity of molluscan hemocyanins from *Helix* and *Rapana* snails. Curr Pharm Biotechnol. 2016;17(3):263–270.
[22] Moltedo B, Faunes F, Haussmann D, et al. Immunotherapeutic effect of Concholepas hemocyanin in the murine bladder cancer model: evidence for conserved antitumor properties among hemocyanins. J Urol. 2006;176(6):2690–2695.
[23] Arancibia S, Espinoza C, Salazar F, et al. A novel immunomodulatory hemocyanin from the limpet Fissurella latimarginata promotes potent anti-tumor activity in melanoma. PloS one. 2014;9(1):e87240. DOI: 10.1371/journal.pone.0087240
[24] Zhong T-Y, Arancibia S, Born R, et al. Hemocyanins stimulate innate immunity by inducing different temporal patterns of proinflammatory cytokine expression in macrophages. J Immunol. 2016;196(11):4650–4662.
[25] Zheng L, Zhao X, Zhang P, et al. Hemocyanin from shrimp *Litopenaeus vannamei* has antiproliferative effect against HeLa cell *in vitro*. PloS One. 2016;11(3):e0151801. DOI: 10.1371/journal.pone.0151801
[26] Dolashka P, Velkova L, Iliev I, et al. Antitumor activity of glycosylated molluscan hemocyanins via Guerin ascites tumor. Immunol Invest. 2011;40(2):130–149.
[27] Dolashka-Angelova P, Stefanova T, Livaniou E, et al. Immunological potential of *Helix vulgaris* and *Rapana venosa* hemocyanins. Immunol Invest. 2008;37(8):822–840.
[28] Antonova O, Yossifova L, Staneva R, et al. Changes in the gene expression profile of the bladder cancer cell lines after treatment with *Helix lucorum* and *Rapana venosa* hemocyanin. J BUON. 2015;20(1):180–187.
[29] Jacobs BL, Lee CT, Montie JE. Bladder cancer in 2010: how far have we come? CA Cancer J Clin. 2010;60(4):244–272.
[30] Li C, Li H, Zhang T, et al. Discovery of Apo-A1 as a potential bladder cancer biomarker by urine proteomics and analysis. Biochem Biophys Res Commun. 2014;446(4):1047–1052.
[31] Chen Y-T, Chen C-L, Chen H-W, et al. Discovery of novel bladder cancer biomarkers by comparative urine proteomics using iTRAQ technology. J Proteome Res. 2010;9(11):5803–5815.
[32] Antonova O, Toncheva D, Rammensee H-G, et al. In vitro antiproliferative effect of *Helix aspersa* hemocyanin on multiple malignant cell lines. Zeitschrift für Naturforschung C. 2014;69(7-8):325–334.
[33] Boyanova O, Dolashka P, Toncheva D, et al. In vitro effect of molluscan hemocyanins on CAL-29 and T-24 bladder cancer cell lines. Biomed Rep. 2013;1(2):235–238.
[34] Stenzl A, Dolashki A, Stevanovic S, et al. Cytotoxic effects of *Rapana venosa* hemocyanin on bladder cancer permanent cell lines. J US-China Med Sci. 2016;13:179–188.
[35] De Smet L, Dimitrov I, Debyser G, et al. The cDNA sequence of three hemocyanin subunits from the garden snail *Helix lucorum*. Gene. 2011;487(2):118–128.
[36] Velkova L, Dimitrov I, Schwarz H, et al. Structure of hemocyanin from garden snail *Helix lucorum*. Comp Biochem Physiol B Biochem Mol Biol. 2010;157(1):16–25.
[37] Dolashka-Angelova P, Schwarz H, Dolashki A, et al. Oligomeric stability of *Rapana venosa* hemocyanin (RvH) and its structural subunits. Biochim Biophys Acta. 2003;1646(1):77–85.
[38] Velkova L, Dolashki A, Dolashka P. Carbohydrate structure of molluscan hemocyanins from snails *Helix lucorum* and *Rapana venosa*, determined by mass spectrometry. J. BioSci. Biotechnol. 2015, SE/ONLINE:75–85.
[39] Stepan A, Ciuca M, Simionescu C, et al. Immunoexpression of N-cadherin, twist and vimentin in bladder urothelial carcinomas. Curr Health Sci J. 2015; 41(3):219–226.
[40] Tyan YC, Yang MH, Chen SCJ, et al. Urinary protein profiling by liquid chromatography/tandem mass spectrometry: ADAM28 is overexpressed in bladder transitional cell carcinoma. RCM 2011;25(19):2851–2862.
[41] Zhao J, Dong D, Sun L, et al. Prognostic significance of the epithelial-to-mesenchymal transition markers e-

cadherin, vimentin and twist in bladder cancer. Int Braz J Urol. 2014;40(2):179–189.

[42] Horvatovich P, Bischoff R, editors. Comprehensive biomarker discovery and validation for clinical application. London (UK): Royal Society of Chemistry; 2013. DOI: 10.1039/9781849734363

[43] Song Y, Luo Q, Long H, et al. Alpha-enolase as a potential cancer prognostic marker promotes cell growth, migration, and invasion in glioma. Mol Cancer. 2014;13:65. DOI: 10.1186/1476-4598-13-65

[44] Liu K, Tang Z, Huang A, et al. Glyceraldehyde-3-phosphate dehydrogenase promotes cancer growth and metastasis through upregulation of SNAIL expression. Int J Oncol. 2017;50(1):252–262.

[45] Yang N, Feng S, Shedden K, et al. Urinary glycoprotein biomarker discovery for bladder cancer detection using LC/MS-MS and label-free quantification. Clin Cancer Res. 2011;17(10):3349–3359.

[46] Nicolas E, Parisot P, Pinto-Monteiro C, et al. Involvement of human ribosomal proteins in nucleolar structure and p53-dependent nucleolar stress. Nat Commun. 2016;7:11390. DOI: 10.1038/ncomms11390

[47] Fan N-J, Kang R, Ge X-Y, et al. Identification alpha-2-HS-glycoprotein precursor and tubulin beta chain as serology diagnosis biomarker of colorectal cancer. Diagn Pathol. 2014;9:53. DOI: 10.1186/1746-1596-9-53

[48] Dieplinger H, Ankerst DP, Burges A, et al. Afamin and apolipoprotein A-IV: novel protein markers for ovarian cancer. Cancer Epidemiol Biomarkers Prev. 2009;18(4):1127–1133.

[49] Zamanian-Daryoush M, DiDonato JA. Apolipoprotein AI and cancer. Front Pharmacol. 2015;6:265. DOI: 10.3389/fphar.2015.00265